

Temporal-Order Judgment of Audiovisual Events Involves Network Activity Between Parietal and Prefrontal Cortices

Bhim Mani Adhikari,¹ Eli S. Goshorn,^{1,2} Bidhan Lamichhane,¹ and Mukesh Dhamala^{1,3}

Abstract

Our perception of the temporal order of everyday external events depends on the integrated sensory information in the brain. Our understanding of the brain mechanism for temporal-order judgment (TOJ) of unisensory events, particularly in the visual domain, is advanced. In case of multisensory events, however, there are unanswered questions. Here, by using physically synchronous and asynchronous auditory–visual events in functional magnetic resonance imaging (fMRI) experiments, we identified the brain network that is associated with the perception of the temporal order of multisensory events. The activation in the right temporo-parietal junction was modulated by the perception of asynchronous audiovisual events. During this perception of temporal order, the right dorsolateral prefrontal cortex coordinated activity with the right temporo-parietal and the left inferior parietal cortices. These results suggest that the TOJ in the multisensory domain underlies a network activity between parietal and prefrontal cortices unlike the regional activity in the right temporo-parietal junction in the unisensory visual domain.

Key words: brain connectivity; effective connectivity; functional connectivity; regions of interest

Introduction

TEMPORAL ORDERING of multisensory events is a common human activity in everyday life. The brain is capable of processing temporal information over a sub-second time scale for sensory and motor functions (Mauk and Buonomano, 2004). Poor temporal information processing is the hallmark of many neurological and psychiatric conditions (Buhusi and Meck, 2005), including dyslexia, schizophrenia, autism, and attention-deficit disorders. Temporal-order judgment (TOJ) tasks, which investigate processing times of information in different modalities, require indicating which of two sequential stimuli was presented first. A typical TOJ task consists of a pair of target stimuli presented with varying stimulus onset asynchronies (SOAs), and participants are asked to judge and indicate the temporal sequence of stimuli which appeared first.

Humans are able to make accurate judgments, when two sensory stimuli occur, were separated in time by 20–50 ms (Poppel, 1997). Recently, using functional magnetic resonance imaging (fMRI), Davis et al. (2009) reported that bilateral temporal parietal junctions (TPJs) were activated during judgments of the temporal order of two visual stimuli. Patients

with damage to left temporo-parietal cortices exhibited impaired TOJ performance (Wittman et al., 2004). Numerous studies suggested that right temporo-parietal structures might likewise play a role in TOJ performance. Another recent study (Woo et al., 2009) reported that transcranial magnetic stimulation (TMS) of the right, but not left, posterior parietal cortex impaired visual TOJ performance when applied 50 or 100 ms post-stimulus onset. Other study showed the right-lateralized structures and their associated role in attention in influencing TOJ performance (Eagleman, 2008). Bernasconi et al. (2010a, 2010b) demonstrated the importance of activity in the posterior sylvian regions in auditory TOJ by investigating auditory-evoked potentials. Recently, brain regions involved in judgments of temporal order of two tactile stimuli were examined (Takahashi et al., 2013), and authors purposed that the temporal order of tactile signals could be determined by combining spatial representations of stimuli in the parietal and prefrontal cortices (Macaluso and Driver, 2005).

However, in the auditory–visual sensory domain, how the brain achieves judgment of temporal order, what brain regions are activated, how activities of these regions are coordinated, and formed accurate asynchrony perception remain

¹Department of Physics and Astronomy, Georgia State University, Atlanta, Georgia.

²Oberlin College, Oberlin, Ohio.

³Center for Behavioral Neuroscience, Institute of Neuroscience, Georgia State University, Atlanta, Georgia.

unknown. To examine the mechanism of TOJ, brain regions, and their role in network interaction, we reanalyzed previously collected fMRI data from experiments on multisensory perception (Dhamala et al., 2007) for audiovisual asynchrony condition, an extension of Davis et al. (2009) TOJ study to the multisensory domain. Using a simple testing protocol composed of beeps and flashes, we investigated the brain regions involved in TOJ. We hypothesized that the TOJ in the audiovisual domain would involve the left and right TPJ, the inferior parietal lobule (IPL), and the dorsolateral prefrontal cortex (DLPFC) based on previous studies on unisensory TOJ (Davis et al., 2009), audio-visual asynchrony perception (Bushara, 2001), multisensory perception (Calvert and Thesen, 2004), and perceptual categorical judgment or decision making (Heekeren et al., 2008). We also hypothesized that the mechanism of TOJ in audiovisual sensory domain would involve the network activity among temporo-parietal and frontal cortices, yielding a subjective order of events in time to a participant.

Materials and Methods

Georgia State University Institutional Review Board approved the protocol for the reanalysis of the fMRI data previously collected and reported in Dhamala et al. (2007). In the original experiments, 12 participants aged between 25 and 37 with no history of psychiatric or neurological disease participated. Participants were first familiarized with the testing procedure in a training session. A behavioral experiment that took place outside the scanner was then conducted to determine which conditions produced the most stable percepts. Besides taking place outside the scanner, the behavioral experiment followed the same protocol as the imaging experiment.

Participants were subjected to sounds (beeps) and light flashes (task paradigm is shown in Fig. 1). SOA and stimulation rate were manipulated as independent variables for a total of 59 different testing conditions in the behavioral experiment. Participants were asked to describe the percept as simultaneous (S) if they had perceived the tone and flash as synchronized events throughout the run, auditory stimuli preceding visual stimuli (AV), visual stimuli preceding auditory stimuli (VA), or “can’t tell” (drift). The auditory stimulus consisted of a 440-Hz–30-ms tone, while the visual stimulus consisted of a 30-ms flash of red light. These stimuli were delivered through a pair of earphones and goggles while the subject was in the scanner.

The imaging experiment employed six unimodal conditions comprising only auditory or visual stimuli and seven bimodal conditions with both types of stimuli. These conditions were selected, because they consistently produced stable percepts in the behavioral experiment; the results from the behavioral experiment are shown in Figure 1 depicted earlier. Stimulation rates of 0.5, 1.5, and 3.0 Hz were used with the SOAs (–200, 0, 200), 0, and (–100, 0, 100) ms between auditory tone and visual flash onsets.

Participants lay supine in the scanner. The testing was done in three runs. In runs 1 and 2, participants were instructed to perceive the auditory and visual stimuli as simultaneous events. Thirteen conditions were tested in a random order, with each condition appearing thrice during the course of the run. A single condition consisted of a 24-sec

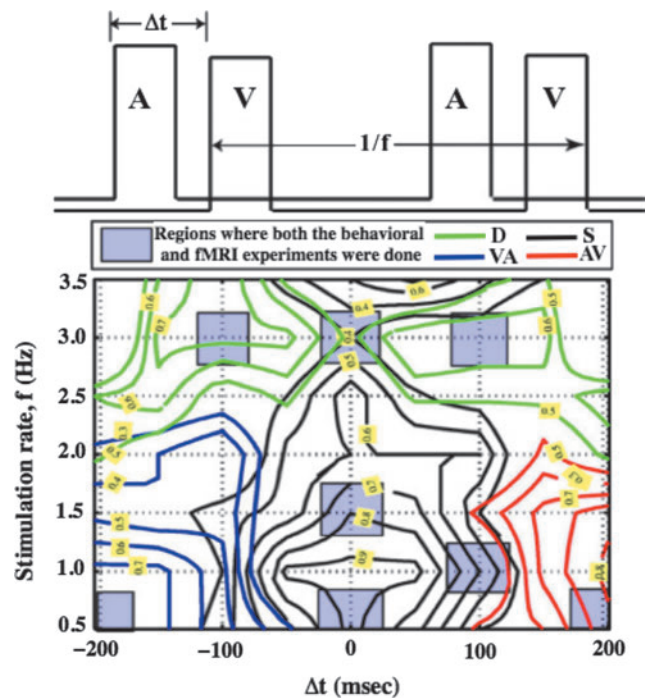


FIG. 1. Experimental design and results from behavioral experiment. The two independent variables, stimulus onset asynchrony and frequency, are represented here as Δt and f . The black lines represent the synchrony percept, while the blue and red lines represent the video-preceding-audio and audio-preceding-video percepts, respectively. The green line represents the drift percept, in which participants reported the two stimuli moving in or out of synchrony.

on-block followed by an 18-sec off-block. Run 1 and 2 lasted 27.3 min. Run 3 lasted 9 min., testing only two bimodal conditions with an SOA of 100 ms and a stimulation rate of 1.0 Hz. An identical design was used, except each block was repeated six times instead of three. A 3-sec visual cue immediately before the testing block directed participants to perceive the stimuli as simultaneous or in AV sequence.

Structural and functional T₁-rated EPI images were acquired from a 1.5-Tesla GE Signa scanner. Five hundred forty-six images per participants were acquired in each of the first two runs, and 180 images per participant were acquired in the third run. Image acquisition parameters were as follows: echo-planar imaging, gradient recalled echo, TR=3000 ms, TE=40 ms, flip angle=90°, 64×64 matrix, and 30 axial slices, each 5 mm thick acquired parallel to the anterior–posterior commissural line.

fMRI data analysis

Data collected in this experiment were preprocessed and analyzed using Statistical Parametric Mapping (SPM8) [Wellcome Trust, London, United Kingdom; (Friston et al., 1995)]. Motion correction was performed using a six-parameter rigid-body transformation to all of the 12 participants included in the analysis. All participants had less than 4 mm of translational and 1° of rotational motion. Four subjects had more than 2 mm of translation in any one direction and more than 2° of rotation about any one of the three axes in

one functional run. We used the framewise displacement procedure (Power et al., 2012) to evaluate the effect of head motion in these four participants and to rule out any possible confounding effects due to head motion. The mean of the motion-corrected images was co-registered to the individual's 30-slice structural image using a 12-parameter affine transformation. The images were spatially normalized to the Montreal Neurological Institute (MNI) template (Talairach and Tournoux, 1988) by applying a 12-parameter affine transformation, then underwent a nonlinear warping using basis functions (Ashburner and Friston, 1999). Images were then smoothed with an 8-mm isotropic Gaussian kernel and high-pass filtered (high-pass filter cut-off of 128 sec) in the temporal domain to remove a very low-frequency trend. A random effect, model-based, statistical analysis was performed with SPM8 in a two-level procedure. At the first level, a separate general linear model (GLM) of the form: $Y = X\beta + \varepsilon$, was specified for each participant, where $X = [1, x_1, x_2, \dots]$, $\beta = [\beta_1, \beta_2, \dots]$, and $\varepsilon = N(0, \sigma^2)$. In the GLM model, $X = [1, x_1, x_2, \dots]$ was a design matrix that included different stimulation conditions (each condition consists of a series of zeros for the off-block and ones for the on-block) in each functional run and time courses of six motion parameters. β 's are the associated effect sizes of X , and ε represents the unexplained variance term. There were 13 stimulation conditions (6 unimodal and 7 bimodal), a total of 13 regressors in runs 1 and 2. In run 3, there were two bimodal conditions and a visual cue, so there was a total of three regressors. All stimulation conditions were convolved with canonical hemodynamic response function. These individual contrast images were then entered into a second-level analysis, using a separate one-sample t -test. The resulting summary statistical maps were overlaid on a high-resolution structural image in MNI orientation for displaying fMRI activations. An inter-regional correlation analysis and network analysis was performed to determine the networks of interdependent brain areas underlying audio-preceding-visual asynchrony perception. Nonparametric Granger causality (GC) (Dhamala et al., 2008a) was used for the network activity analysis.

Connectivity (network) analysis

The regions of interest (ROIs) were based on activation t -maps. We defined spherical masks using MarsBaR (Brett et al., 2002). The voxel that had the highest statistical value was selected as the center of the mask. Here, the defined masks were centered at the right middle frontal gyrus (45, 32, 37), right TPJ (45, -58, 28), and left IPL (-57, -52, 43), called ROIs DLPFC, TPJ, and IPL, respectively. Each spherical ROI mask was of 6 mm radius. Signal time courses from all voxels were extracted from each ROI for all subjects. The signal time courses were cut and, hence, collected as trials for asynchrony perceptions. The ensemble-mean removed segmented timeseries from separate voxels, task blocks (for stimulus on period only) and subjects were treated as trials for reliable estimates of the network measures.

Functional connectivity

Average time series for a trial was calculated for each subject from all ROIs. We then calculated the pairwise correlation coefficients from trial to trial between two ROIs. To estimate the average effect, we used Fisher's z -transformation (Bond

and Richardson, 2004; Cox, 2008; Silver and Dunlap, 1987) on cross-correlation values. The correlation coefficients were converted to their equivalent Fisher's z -values ($z = \arctan h(r)$) to compute average Fisher's z -value. The average Fisher's z -values for each subject, and each pair of ROIs were then used to calculate the grand average z -value, the significance level p , and the corresponding correlation coefficient.

Directed functional connectivity

The voxel time series data for each ROI were segmented for audiovisual asynchrony perception. Each segment was 24 sec long, and there were 360 segments for each subject, a total of 4320 segments as trials. Temporal mean from each trial and ensemble mean from all trials were taken out, and frequency-dependent nonparametric GC spectra (Dhamala et al., 2008a) for pairs of ROIs were calculated. From causality values, the time-domain GC causality was obtained by integrating the causality spectra over the entire frequency range. The significant GC spectra were defined by setting a GC threshold above the random-noise baseline. To compute the threshold value of GC, we constructed two sets of surrogates for each subject and used the random permutation technique (Blair and Karniski, 1993; Brovelli et al., 2004). The first set of surrogate data were constructed by randomly permuting trials from activated voxels, and the second set was constructed by permuting segments of randomly selected nonactivated voxels of the brain. The threshold was, thus, based on the null hypothesis that there was no statistical interdependence between two nodes when trials were randomized or selected from nonactivated voxels. The trial-randomized surrogate data from activated voxels provided an estimate of expected GC not associated with the task. The surrogate data from nonactivated voxels provided an estimate of expected GC with baseline physiological influences regardless of the task. We computed GC spectra from all possible pairs of ROIs with 250 random permutations and picked maximum GC on each permutation. By fitting the distribution with gamma-distribution function (Dhamala et al., 2008a), we obtained the threshold for GC spectra at significance $p < 10^{-3}$. This threshold GC was used to identify significantly active directed network activity among three ROIs: right DLPFC, right TPJ, and left IPL. We computed the time-domain GC values for significantly active network directions. Finally, the GC spectra and then time-domain GC were calculated from all subjects in order to evaluate the differential network activities between audiovisual asynchrony and synchrony perception conditions.

Results

The fMRI activation analysis with SPM8 was used to look at the activation maps when participants perceived temporal asynchrony and when they perceived synchrony for auditory leading visual (AV) stimuli. Random-effects analysis of the AV asynchrony versus rest condition showed activations in the right superior temporal gyrus (STG), IPL and supramarginal gyrus (TPJ); left medial frontal gyrus (MeFG), right middle frontal gyrus within DLPFC, and left IPL shown in Figure 2. These activations were initially subjected to a cluster-forming threshold $p < 0.001$ (uncorrected) and cluster size, $k > 20$ for AV asynchrony stimulation conditions. We performed multiple-comparisons correction on all the activation t -maps

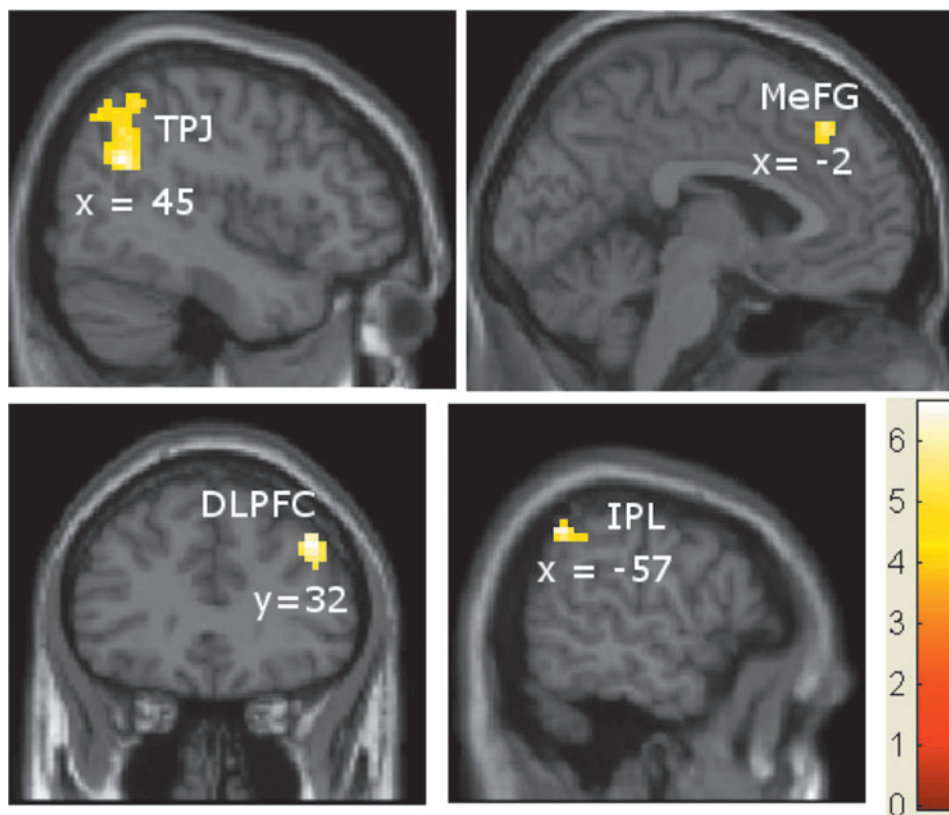


FIG. 2. Activations related to auditory leading visual (AV) asynchrony perceptions cluster-based family wise error correction ($p < 0.05$). Areas: temporal parietal junction [TPJ] includes right superior temporal gyrus, inferior parietal lobe (IPL) and supramarginal gyrus], medial frontal gyrus (left MeFG), dorsolateral prefrontal cortex (DLPFC includes right middle frontal gyrus, BA 9), and IPL (left IPL). The color intensity represents t -statistics, and the activations are overlaid on the Montreal Neurological Institute structural template brain in neurological orientation.

using AlphaSim procedure in AFNI (Cox, 1996; B.D. Ward, <http://afni.nih.gov/afni/docpdf/AlphaSim.pdf>). All of the activations survive significance of corrected $p < 0.05$, as shown in Table 1(a). Table 1(b) shows the brain activations related to auditory leading visual (AV) synchrony perceptions (a cluster-based family wise error correction, $p < 0.05$). The areas are left STG, including IPL, left superior frontal gyrus (SFG), and right STG. These areas are shown in rendered brain in Figure 3; the clusters of fMRI voxels more significantly activated by audiovisual asynchrony perception > rest (in green color) and synchrony perception > rest (in red color).

From this study, we found that left temporal and parietal cortices as well as right frontal cortex are involved in the synchrony perception. Asynchrony perception auditory leading visual stimuli, whereas we observed right temporal and parietal cortices, TPJ, and right frontal cortex plus left parietal cortex (IPL) involved. Involvement of TPJ for TOJ tasks matches with the earlier study by Davis et al. (2009) in the unisensory visual domain. They found the brain activations on both right and left TPJ in TOJ task. In order to explore whether left/right TPJ is involved in TOJ task in the multisensory audiovisual domain, we used the activation coordinates from this previous work, and selected two spherical ROIs (shown atop of Fig. 4), each of radius 6 mm, from right TPJ centered at (64, -50, and 14) and left TPJ centered at (-50, -48, and 10). The time-courses data were also analyzed in a correlation/regression analysis; in which region-specific beta values were computed from each subject and were averaged to produce average β values from ROIs mentioned earlier for asynchrony and synchrony perceptions. We performed a paired t -test (i) within an ROI for different stimulation conditions (ii) across ROIs for the same stimulation conditions, and (iii) across

ROIs for different stimulation conditions. We found the average β values significant for right and left TPJ for asynchrony perception ($p = 0.006$) with higher values in the right TPJ, but not significant for synchrony perception ($p = 0.368$). The average β in the right TPJ tended to be significant for synchrony perception (uncorrected $p = 0.054$). Figure 4 showed the results of this analysis and Table 2, the statistical value obtained from paired t -test. Moreover, average β values from left TPJ were found significant ($p = 0.017$) for synchrony perception.

We performed connectivity analysis among these activation regions. Inter-regional correlation analysis, as described earlier, was used to see whether these regions were functionally connected. Figure 5(A) shows the functional connectivity, indicating that there was a functional linkage between R DLPFC and L IPL ($r = 0.410$, $p = 0.019$); L IPL and R TPJ ($r = 0.357$, $p = 0.040$); and R TPJ and R DLPFC ($r = 0.413$, $p = 0.018$). Figure 5(B) shows the directed functional connectivity obtained by nonparametric GC analysis for audiovisual asynchrony perception. In synchrony condition, we found the similar connectivity patterns, but the strengths were much reduced (not shown). L IPL received strong causal influences from R DLPFC and R TPJ, the former being the strongest. The causal interaction between R DLPFC and R TPJ was found to be bidirectional. The displayed values are time-domain GC values; the maximum time-domain value found was 0.04, and maximum GC value obtained during calculation was 0.0192. Figure 5(C) shows the structural connectivity constructed from CoCoMac database (Ghosh et al., 2008; Kotter and Wanke, 2005; Stephan et al., 2000). The functional and directed functional connectivity patterns are consistent with the underlying structural connectivity between these brain regions. Figure 6 shows the time-domain GC values for

TABLE 1. SIGNIFICANT BRAIN ACTIVATIONS FOR ASYNCHRONY PERCEPTION (A) AND FOR SYNCHRONY PERCEPTION (B)

| (a) | | | | |
|--|------------------|--------------|-------------|-------------------------|
| Contrast | Cluster size | Brain areas | T (z-score) | MNI coordinates x, y, z |
| Asynchrony audio-preceding-visual > rest | 311 ^a | R STG | 6.61 (4.12) | 45, -58, 28 |
| | | R IPL | 6.18 (3.98) | 48, -58, 40 |
| | | R SmG | 5.18 (3.61) | 57, -46, 37 |
| | 82 ^a | R MFG | 5.43 (3.71) | 45, 32, 37 |
| | | RMFG | 4.13 (3.14) | 45, 14, 49 |
| | 40 ^b | L MeFG | 6.44 (4.07) | -2, 35, 46 |
| | 36 ^b | L IPL | 6.32 (4.03) | -57, -52, 43 |
| | | L IPL | 4.93 (3.51) | -60, -43, 40 |
| (b) | | | | |
| Synchrony audio-preceding-visual > rest | 54 ^a | L STG | 8.00 (4.51) | -57, -61, 25 |
| | | L IPL | 4.11 (3.14) | -48, -64, 40 |
| | 20 ^b | R STP | 5.79 (3.84) | 69, -25, 16 |
| | | RSTG | 4.13 (3.14) | 60, -25, 13 |
| | 20 ^b | L SFG (BA 9) | 5.67 (3.80) | -18, 56, 31 |
| 12 ^b | L SFG (BA 6) | 5.06 (3.56) | -15, 26, 61 | |

The t-map of each contrast was corrected for multiple comparisons using the AlphaSim command in AFNI (Cox, 1996; B. D. Ward, <http://afni.nih.gov/afni/docpdf/AlphaSim.pdf>). The individual voxel threshold probability threshold was set to be 0.05.

^a $p < 0.001$.

^b $p < 0.05$ (AlphaSim correction).

L, left; R, right; STG, superior temporal gyrus; IPL, inferior parietal lobule; SmG, supramarginal gyrus; MFG, middle frontal gyrus; MeFG, medial frontal gyrus; STP, superior parietal pole; SFG, superior frontal gyrus; MNI, Montreal Neurological Institute.

asynchrony and synchrony perception conditions computed from all subjects. The directed functional connectivity was significantly stronger ($p < 0.01$) in asynchrony than in synchrony perception conditions from R DLPFC to L IPL and R TPJ to R DLPFC.

Discussion

Our results suggest that a network of areas comprising prefrontal, sensory, and parietal cortices establishes the perception of asynchrony, which is consistent with the foregoing research. The audiovisual asynchrony percept versus rest contrast shows the significant brain activations in right TPJ, right DLPFC, left IPL, and left MeFG. The connectivity analyses showed that the right DLPFC coordinated activity with the right temporo-parietal and the left inferior parietal cortices during the perception of audiovisual asynchrony. These findings in multisensory domain plus the previous findings in the visual domain reported by Davis et al. (2009) advance our understanding of brain mechanisms for temporal asynchrony.

The prefrontal cortex was found to be involved in almost all high-level cognitive tasks such as working memory, memory retrieval, and perceptual priming tasks. Prefrontal activations were mostly right lateralized during sustained attention and episodic retrieval; were left lateralized during language, semantic memory retrieval, and memory encoding; and were bilateral during working memory. Cognitively controlled timing caused the right hemispheric DLPFC to be more active frequently than any other brain region (Lewis and Miall, 2003). Neuropsychological study (Koch et al., 2002), neuroimaging study (Rubia and Smith, 2004) have shown the involvement of right hemispheric DLPFC in timing tasks. Lesions to this area plus inferior parietal cortex have been shown to disrupt cognitive timing (Harrington et al., 1998). Moreover, the differential involvement of the right DLPFC in cognitive and automatic timing has been supported by a TMS study showing impaired reproduction of suprasedond, more cognitive; but not subsecond, more automatic; intervals (Jones et al., 2004). Koch et al. (2002) showed that repetitive TMS to the right but not left DLPFC disrupts the timing of suprasedond durations. Since the prefrontal cortex was involved in working memory and cognitive timing, Lewis and Miall (2006) purposed it as a multipurpose processor recruiting for a wide variety of functions. The greater changes in signal intensity

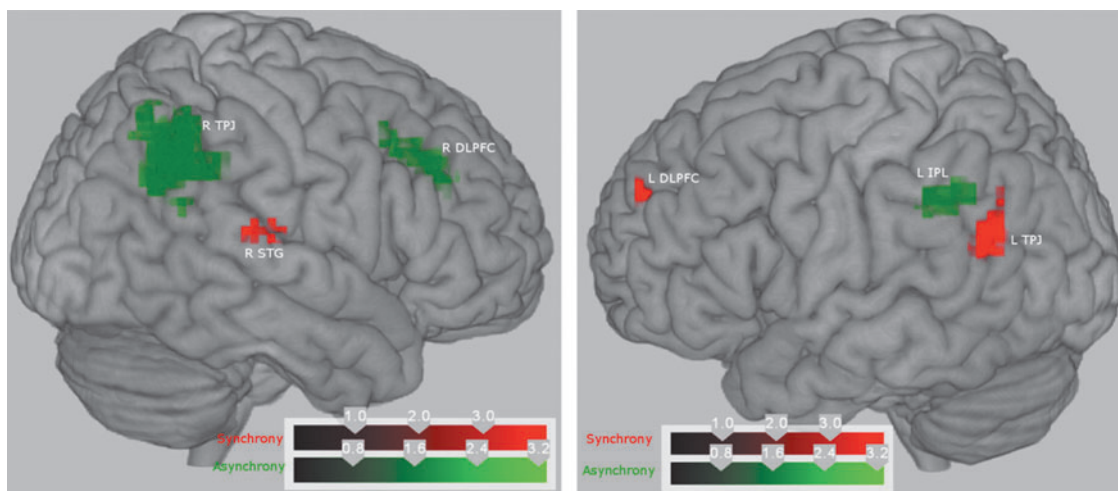


FIG. 3. Brain renderings displaying the z-scores of clusters of functional magnetic resonance imaging voxels more significantly activated by audiovisual asynchrony perception > rest (green) and synchrony perception > rest (red). Left, Sagittal rendering of the right hemisphere. Right, Sagittal rendering of the left hemisphere.

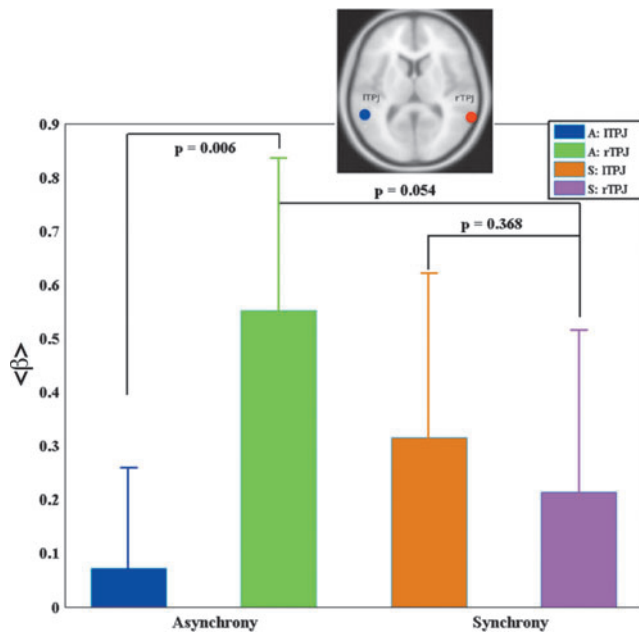


FIG. 4. Mean contrast values: Contrast values were calculated for both asynchrony (A) and synchrony (S) perceptions from right temporal parietal junction (rTPJ) and left temporal parietal junction (ITPJ) regions of interest (ROIs are shown atop) from each subject and were used to calculate mean beta and the standard error of the mean.

from MeFG were found during where condition in the right hemisphere than the left; whereas it was more to the left hemisphere during when and what conditions (Talati and Hirsch, 2005). For each sensory modality: visual, tactile, or auditory, where condition is biased toward the right hemisphere; whereas when condition was biased toward the left hemisphere, hence, the left hemisphere of the MeFG was engaged for processing of perceptual decisions based on when and what information whereas the decisions on the right hemisphere were based on where information.

Severe and prolonged spatial deficits were more common in right hemisphere patients. A supporting evidence for the involvement of right, not the left, hemisphere in the detection of temporal events was described using flicker paradigm (Battelli et al., 2003). They reported that the impaired performance was in detecting whether an item is flickering

out of phase with its neighbors in three patients with right parietal injury but relatively normal performance in the other three individuals who had left parietal injury (Battelli et al., 2003). Battelli et al. (2007) stated that right parietal lobe serves as a part of a when pathway for visual stimuli and with compromised judgment of temporal order, simultaneity, and high-level motion after right parietal lesions or degraded with TMS over right parietal but not elsewhere. Right parietal patients without neglect (Shapiro et al., 2002) have shown a prolonged and severe impairment in the orienting of attention in time. An fMRI study has shown that the right parietal cortex is transiently active when attention shifts between spatial locations (Yantis et al., 2002) or during tasks in which targets are presented at unexpected locations (Corbetta et al., 2000). The absence of such a deficit in left parietal patients' comparatively similar lesions in the right parietal strongly suggested that the right parietal lobe was specialized in determining when objects appear and disappear.

Left inferior parietal cortex, known as a neural substrate of linkages between perception and preparation of action (Rizzolatti and Luppino, 2001), was found to be activated in asynchrony detection and integrating spatiotemporal information (Assmus et al., 2003). Activation of this area was, therefore, associated not only with the difficulty of motor tasks (Winstein et al., 1997), consistent with its important role in the spatiotemporal control of skilled actions (Buxbaum et al., 2003), but also with the difficulty of integrating spatiotemporal information in a perceptual task (Assmus et al., 2005). In a PET study of goal-directed reciprocal aiming, subjects showed a rise in regional cerebral blood flow in distributed cortical regions, including the left inferior parietal cortex (Winstein et al., 1997). A primate study has shown the parietal cortex playing an important role in perception and estimation of time (Leon and Shadlen, 2003), and working along with the prefrontal cortex in temporal interval monitoring (Onoe et al., 2001). Anatomical studies in primates showed that the auditory cortex has neuronal projections to inferior parietal and prefrontal cortices, and prefrontal cortex cells have a clear association with visual and auditory stimuli across time (Fuster et al., 2000). A recent study (Moser et al., 2009) described the role of left IPL in temporal-order processing of syllables. A number of lesion studies showed that patients with right (Baylis et al., 2002; Rorden et al., 1997; Synder and Chatterjee, 2004) and left (Baylis et al., 2002) hemisphere injury exhibit biased performance on the TOJ. TMS over the right, but not the left, parietal cortex delayed the detection of a visual target in the contralateral hemi-field, thus leading to biased TOJ performance (Woo et al., 2009). Meister et al. (2006) observed that the application of single-pulse TMS over right TPJ caused extinction-like performance in a detection task of unilaterally versus bilaterally presented visual stimuli, but had no such effects when TMS was applied over STG. Another study (Grandjean et al., 2008) showed that damage to area TPJ was correlated with the extinction of auditory stimuli.

The event-related fMRI study (Downar et al., 2000) was carried out to find the brain regions responsive to changes in visual, auditory, and tactile stimuli. They found that unimodal activations were bilateral and predominantly to association cortices, whereas multimodal activations were

TABLE 2. THE SIGNIFICANCE LEVEL (P-VALUE AND CORRESPONDING T-VALUE IN PARENTHESES), FOR DIFFERENT COMBINATIONS OF AUDIOVISUAL ASYNCHRONY (A) AND SYNCHRONY (S) PERCEPTIONS BETWEEN ITPJ/rTPJ OBTAINED FROM PAIRWISE T-TESTS

| Conditions and regions used for test | p-Value (t-value) |
|--------------------------------------|-------------------|
| A: ITPJ, A: rTPJ | 0.006 (-3.65) |
| A: ITPJ, S: ITPJ | 0.017 (-2.58) |
| A: ITPJ, S: rTPJ | 0.052 (-2.06) |
| A: rTPJ, S: ITPJ | 0.196 (1.33) |
| A: rTPJ, S: rTPJ | 0.054 (2.03) |
| S: ITPJ, S: rTPJ | 0.368 (0.919) |

ITPJ/rTPJ, left/right temporal parietal junction.

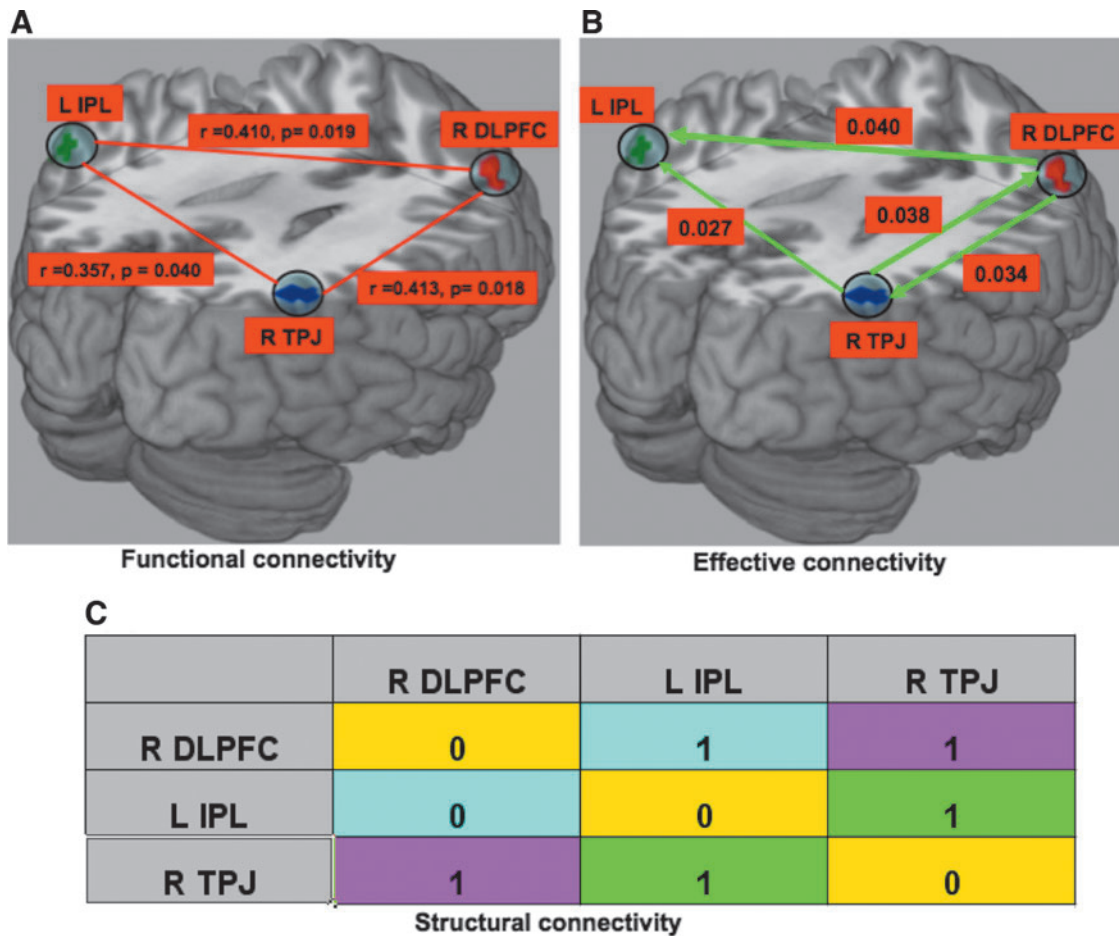


FIG. 5. Connectivity analysis: (A) Functional connectivity, (B) Directed functional connectivity during audiovisual asynchrony perception by nonparametric Granger causality technique, (C) Structural connectivity based on CoCoMac database (Ghosh et al., 2008; Kotter and Wanke, 2005; Stephan et al., 2000) (“0” means there is no structural connection whereas “1” means there is). Here, r represents the correlation coefficient and p represents significance p -value, the probability of observing the given result by chance if the null hypothesis is true. These three regions are functionally connected (cross-correlation analysis) as shown in plot (A). IPL received the strong causal influences from both TPJ and DLPFC, whereas there was bidirectional causal interaction between them, as shown in plot (B).

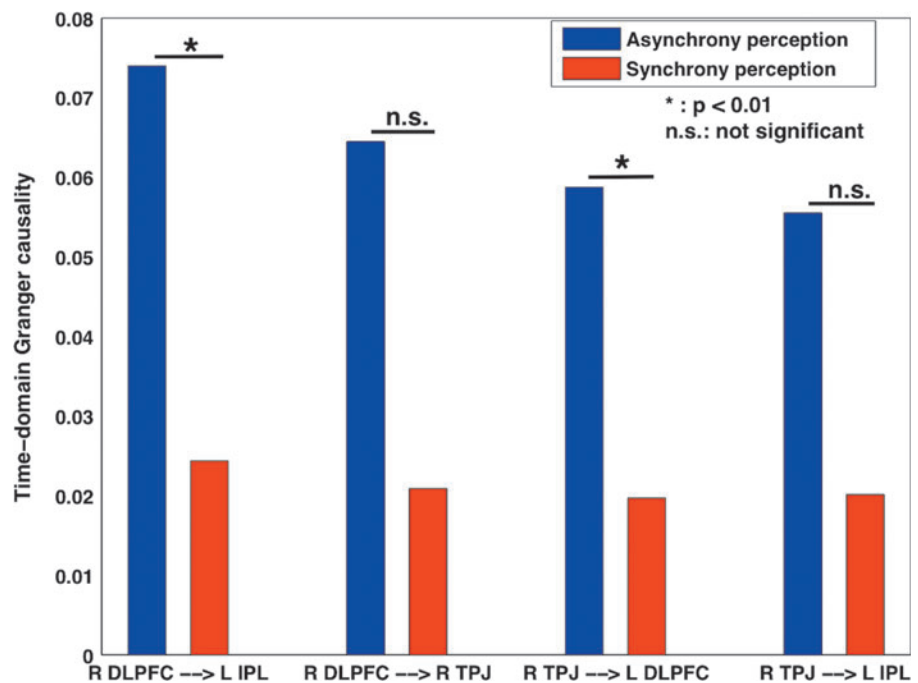


FIG. 6. Directed connectivity in audiovisual asynchrony and synchrony. The causal influences from R DLPFC to L IPL and R TPJ to L DLPFC were significantly greater for asynchrony perception.

strongly lateralized to the right hemisphere, comprising a right-lateralized network, including the temporo-parietal junction, inferior frontal gyrus, insula, and supplementary motor areas. Another study (Matsushashi et al., 2004) used the epicortical recording of evoked responses, in six patients having intractable partial epilepsy who underwent chronic implantation of subdural electrodes in TPJ for presurgical evaluation. This study provided the direct evidence that the human TPJ was involved in the processing of multisensory inputs, including somatosensory, auditory, and visual modalities with no clear hemispheric dominance; may be, it is rarely needed to employ epicortical recording from both sides clinically.

Our regions specific [regions right (R) TPJ and left (L) TPJ were selected from previous study (Davis et al., 2009)] beta-contrast-modulation analysis showed that the R TPJ is more specific to TOJ in the audiovisual multisensory domain. In addition, this analysis showed that the L TPJ activations may be modulated by the audiovisual synchrony percept, supporting the fact that judging temporal synchrony activated a predominantly left hemisphere (Lux et al., 2003). R TPJ involvement for TOJ asynchrony perception seemed to be supported by evidence that the right was more active in the TOJ task than the shape task for visual stimuli (Davis et al., 2009).

As per the existing imaging, electrophysiological and anatomical literature, networks of brain areas, rather than any individual site, have been involved in cross-modal processing even though each component of these networks may have a different contribution to integrating different types of cross-modal information (Calvert et al., 2001). We, therefore, focused not only on the role of individual regions, but also, their contributions in the network for the TOJ in audiovisual multisensory domain. The identified brain activation regions involved in time and space encoding supported our hypothesis that they formed a unified network. Clear and significant functional linkage as seen showed the levels of interdependent between these regions. We performed the connectivity analysis, mainly, concerning the directions of neural interactions and how one neural system exerted influence over another. We here used nonparametric GC technique, which was effectively applied to synthetic data generated by network models (Dhamala et al., 2008b) with known connectivity and to local field potentials recorded from monkeys performing a sensorimotor task (Dhamala et al., 2008a). The nonparametric GC approach is based on the direct Fourier transforms of data that eliminate the need of parametric data modeling. Here, we found the L IPL receiving strong causal influences from R TPJ and R DLPFC for temporal-order asynchrony perception, showed that it is a main hub in the detection of asynchrony and in integrating spatiotemporal information. R TPJ and R DLPFC had bidirectional communication, indicating that these regions are responsible for the temporal order perception. Thus directed functional connectivity analysis suggested that the DLPFC coordinates brain activity with TPJ and IPL in an audiovisual timing percept. Moreover, higher directed connectivity strengths during asynchrony than synchrony perception conditions suggest that the network comprising these nodes is responsible for TOJs in the audiovisual domain. Our findings of brain mechanisms of TOJs in the audiovisual domain and the findings reported by Davis and his colleagues (Davis et al., 2009) in the visual (unisensory) domain together suggest that tempo-

ral judgment mechanism functions independently of sensory modalities and need not be linked to response planning. We believe that the current work focused on the audiovisual domain for temporal-order asynchrony perception can be adapted to further our understanding of integration of information from other sensory modalities (such as touch) and even with the subjects having visual and hearing impairment. Extending these findings to other modalities can help answer the questions whether the same brain network is involved regardless of modality and how the multimodal TOJ could be confirmed.

Acknowledgments

This work was supported by the National Science Foundation (NSF) Grant BCS 0955037 (M.D.). The content of this publication is solely the responsibility of the authors and does not necessarily represent the official views of the NSF. The BRAIN program directed by Dr. Kyle Franz at the Center for Behavioral Neuroscience, Georgia State University provided a summer fellowship to the author E.G. M.D. would also like to extend sincere thanks to Drs. Viktor Jirsa, Collins Assisi and Scott Kelso for all the scientific discussions during the previous study (Dhamala et al., NeuroImage, 2007).

Author Disclosure Statement

There is no conflict of interest for any of the authors.

References

- Ashburner J, Friston KJ. 1999. Nonlinear spatial normalization using basis functions. *Hum Brain Mapp* 7:254–266.
- Assmus A, Marshall JC, Noth J, Zilles K, Fink GR. 2005. Difficulty of perceptual spatiotemporal integration modulates the neural activity of left inferior parietal cortex. *Neuroscience* 132:923–927.
- Assmus A, Marshall JC, Ritzl A, Noth J, Zilles K, Fink GR. 2003. Left inferior parietal cortex integrates time and space during collision judgments. *Neuroimage* 20:S82–S88.
- Battelli L, Cavanagh P, Martini P, Bartyon JJ. 2003. Bilateral deficits of transient visual attention in right parietal patients. *Brain* 126:2164–2176.
- Battelli L, Pascual-Leone A, Cavanagh P. 2007. The ‘when’ pathway of the right parietal lobe. *Trends Cogn Sci* 11:204–210.
- Baylis GC, Simon SL, Baylis LL, Rorden C. 2002. Visual extinction with double simultaneous stimulation: what is simultaneous? *Neuropsychologia* 40:1027–1034.
- Bernasconi F, Grivel J, Murray MM, Spierer L. 2010a. Interhemispheric coupling between the posterior sylvian regions impacts successful auditory temporal order judgment. *Neuropsychologia* 48:2579–2585.
- Bernasconi F, Grivel J, Murray MM, Spierer L. 2010b. Plastic brain mechanisms for attaining auditory temporal order judgment proficiency. *Neuroimage* 50:1271–1279.
- Blair RC, Karniski W. 1993. An alternative method for significance testing of waveform difference potentials. *Psychophysiology* 30:518–524.
- Bond CF, Richardson K. 2004. Seeing the Fisher z-transformation. *Psychometrika* 69:291–303.
- Brett M, Anton JL, Valabregue R, Poline JB. 2002. Region of interest analysis using an SPM toolbox [abstract]. In Presented at the 8th International Conference on Functional Mapping of the Human Brain, Sendai, Japan.

- Brovelli A, Ding M, Ledberg A, Chen Y, Nakamura R, Bressler SL. 2004. Beta oscillations in a large-scale sensorimotor cortical network: directional influences revealed by Granger causality. *Proc Natl Acad Sci USA* 101:9849–9854.
- Buhusi CV, Meck WM. 2005. What makes us tick? Functional and neural mechanisms of interval timing. *Nat Rev Neurosci* 6:755–765.
- Bushara KO. 2001. Neural correlates of auditory-visual stimulus onset asynchrony detection. *J Neurosci* 21:300–304.
- Buxbaum LJ, Sirigu A, Schwartz MF, Klatzky R. 2003. Cognitive representations of hand posture in ideomotor apraxia. *Neuropsychologia* 41:1091–1113.
- Calvert GA, Hansen PC, Iversen SD, Brammer MJ. 2001. Detection of audio-visual integration sites in humans by application of electrophysiological criteria to the BOLD effect. *Neuroimage* 14:427–438.
- Calvert GA, Thesen T. 2004. Multisensory integration: methodological approaches and emerging principles in the human brain. *J Physiol Paris* 98:191–205.
- Corbetta M, Kincade MJ, Ollinger JM, McAvoy MP, Shulman GL. 2000. Voluntary orienting is dissociated from target detection in human posterior parietal cortex. *Nat Neurosci* 3:292–297.
- Cox NJ. 2008. Speaking stata: correlation with confidence, or Fisher's z revisited. *Stata J* 8:413–439.
- Cox RB. 1996. AFNI: software for analysis and visualization of functional magnetic resonance neuroimages. *Comput Biomed Res* 29:162–173.
- Davis B, Christie J, Rorden C. 2009. Temporal order judgments activate temporal parietal junction. *J Neurosci* 29:3182–3188.
- Dhamala M, Assisi CG, Jirsa VK, Steinberg FL, Kelso JA. 2007. Multisensory integration for timing engages different brain networks. *Neuroimage* 34:764–773.
- Dhamala M, Rangarajan G, Ding M. 2008a. Analyzing information flow in brain networks with nonparametric Granger causality. *Neuroimage* 41:354–362.
- Dhamala M, Rangarajan G, Ding M. 2008b. Estimating Granger causality from Fourier and wavelet transforms of time series data. *Phys Rev Lett* 100:018701.
- Downar J, Crawley AP, Mikulis DJ, Davis KD. 2000. A multimodal cortical network for the detection of changes in the sensory environment. *Nat Neurosci* 3:277–283.
- Eggleman DM. 2008. Human time perception and its illusions. *Curr Opin Neurobiol* 18:131–136.
- Friston KJ, Holmes AP, Worsely KJ, Poline J-B, Firth CD, Frackowiak RSJ. 1995. Statistical parametric maps in functional imaging: a general linear approach. *Hum Brain Mapp* 2:189–210.
- Fuster JM, Bodner M, Kroger JK. 2000. Cross-modal and cross-temporal association in neurons of frontal cortex. *Nature* 405:347–351.
- Ghosh A, Rho Y, McIntosh AR, Kotter R, Jirsa VK. 2008. Noise during rest enables the exploration of the brain's dynamic repertoire. *PLoS Comput Biol* 4:e1000196.
- Grandjean D, Sander D, Lucas N, Scherer KR, Vuilleumier P. 2008. Effects of emotional prosody on auditory extinction for voices in patients with spatial neglect. *Neuropsychologia* 46:487–496.
- Harrington DL, Haaland KY, Knight RT. 1998. Cortical network underlying mechanisms of time perception. *J Neurosci* 18:1085–1095.
- Heekeren HR, Marrett S, Ungerleider LG. 2008. The neural systems that mediate human perceptual decision making. *Nat Rev Neurosci* 9:467–479.
- Jones CR, Rosenkranz K, Rothwell JC, Jahanshahi M. 2004. The right dorsolateral prefrontal cortex is essential in time reproduction: an investigation with repetitive transcranial magnetic stimulation. *Exp Brain Res* 158:366–372.
- Koch G, Oliveri M, Carlesimo GA, Caltagirone C. 2002. Selective deficit of time perception in a patient with right prefrontal cortex lesion. *Neurology* 59:1658–1659.
- Kotter R, Wanke E. 2005. Mapping brains without coordinates. *Philos Trans R Soc Lond B Biol Sci* 360:751–766.
- Leon MI, Shadlen MN. 2003. Representation of time by neurons in posterior parietal cortex of the macaque. *Neuron* 38:317–327.
- Lewis PA, Miall RC. 2003. Distinct systems for automatic and cognitively controlled time measurement: evidence from neuroimaging. *Curr Opin Neurobiol* 13:250–255.
- Lewis PA, Miall RC. 2006. Remembering the time: a continuous clock. *Trends Cogn Sci* 10:401–406.
- Lux S, Marchant JL, Ritzl A, Zilles K, Fink GR. 2003. Neural mechanisms associated with attention to temporal synchrony versus spatial orientation: an fMRI study. *Neuroimage* 20:S58–S65.
- Macaluso E, Driver J. 2005. Multisensory spatial interactions: a window onto functional integration in the human brain. *Trends Neurosci* 28:264–271.
- Matsushashi M, Ikeda A, Ohara S, Matsumoto R, Yamamoto J, Takayama M, Satow T, Begum T, Usui K, Nagamine T, Mikuni N, Takahashi J, Miyamoto S, Fukuyama H, Shibasaki H. 2004. Multisensory convergence at human temporo-parietal junction—epicortical recording of evoked responses. *Clin Neurophysiol* 115:1145–1160.
- Mauk MD, Buonomano DV. 2004. The neural basis of temporal processing. *Ann Rev Neurosci* 27:307–340.
- Meister IG, Wienemann M, Buelte D, Grünewald C, Sparing R, Dambeck N, Boroojedi B. 2006. Hemiextinction induced by transcranial magnetic stimulation over the right temporo-parietal junction. *Neuroscience* 142:119–123.
- Moser D, Baker JM, Sanchez CE, Rorden C, Fridriksson J. 2009. Temporal order processing of syllables in the left parietal lobe. *J Neurosci* 29:12568–12573.
- Onoe H, Komori M, Onoe K, Takechi H, Tsukada H, Watanabe Y. 2001. Cortical networks recruited for time perception: a monkey positron emission tomography (PET) study. *Neuroimage* 13:37–45.
- Poppel E. 1997. A hierarchical model of temporal perception. *Trends Cogn Sci* 1:56–61.
- Power JD, Barnes KA, Snyder AZ, Schlaggar BL, Petersen SE. 2012. Spurious but systematic correlations in functional connectivity MRI networks arise from subject motion. *Neuroimage* 59:2142–2154.
- Rizzolatti G, Luppino G. 2001. The cortical motor system. *Neuron* 31:889–901.
- Rorden C, Mattingley JB, Karnath H-O, Driver J. 1997. Visual extinction and prior entry: impaired perception of temporal order with intact motion perception after unilateral parietal damage. *Neuropsychologia* 35:421–433.
- Rubia K, Smith A. 2004. The neural correlates of cognitive time management: a review. *Acta Neurobiol Exp* 64:329–340.
- Shapiro K, Hillstrom AP, Husain M. 2002. Control of visuotemporal attention by inferior parietal and superior temporal cortex. *Curr Biol* 12:1320–1325.
- Silver NC, Dunlap WP. 1987. Averaging correlation coefficients: should Fisher's z transformation be used? *J Appl Psychol* 72:146–148.
- Stephan KE, Hilgetag C-C, Burns GAPC, O'Neill MA, Young MP, Kotter R. 2000. Computational analysis of functional

- connectivity between areas of primate cerebral cortex. *Philos Trans R Soc Lond B Biol Sci* 355:111–126.
- Synder JJ, Chatterjee A. 2004. Spatial-temporal anisometries following right parietal damage. *Neuropsychologia* 42:1703–1708.
- Takahashi T, Kansaku K, Wada M, Shibuya S, Kitazawa S. 2013. Neural correlates of tactile temporal-order judgment in humans: an fMRI study. *Cereb Cortex* 23:1952–1964.
- Talairach J, Tournoux P. 1988. *Co-Planar Stereotaxic Atlas of the Human Brain; 3-D Proportional System: An Approach to Cerebral Imaging*. New York, NY: Thieme Classics.
- Talati A, Hirsch J. 2005. Functional specialization within the medial frontal gyrus for perceptual go/no-go decisions based on “what,” “when,” and “where,” related information: an fMRI study. *J Cogn Neurosci* 17:981–993.
- Winstein CJ, FGrafton ST, Pohl PS. 1997. Motor task difficulty and brain activity: investigation of goal-directed reciprocal aiming using positron emission tomography. *J Neurophysiol* 77:1581–1594.
- Wittman M, Burtscher A, Fries W, von Steinbüchel N. 2004. Effects of brain-lesion size and location on temporal-order judgment. *Neuroreport* 15:2401–2405.
- Woo SH, Kim KH, Lee KM. 2009. The role of the right posterior parietal cortex in temporal order judgment. *Brain Cogn* 69:337–343.
- Yantis S, Schwarzbach J, Serences JT, Carlson RL, Steinmetz MA, Pekar JJ, Courtney SM. 2002. Transient neural activity in human parietal cortex during spatial attention shifts. *Nat Neurosci* 5:995–1002.

Address correspondence to:

Bhim Mani Adhikari

Department of Physics and Astronomy

Georgia State University

25 Park Place, Room 605

Atlanta, GA 30303

E-mail: badhikari1@student.gsu.edu